Published in final edited form as:
Acad Radiol. 2010 December ; 17(12): 1477–1485. doi:10.1016/j.acra.2010.07.009.

Multiparametric Magnetic Resonance Imaging, Spectroscopy and Multinuclear (^{23}Na) Imaging Monitoring of Preoperative Chemotherapy for Locally Advanced Breast Cancer

Michael A. Jacobs, Ph.D.[1,2], **Vered Stearns, M.D.**[2], **Antonio C. Wolff, M.D**[2], **Katarzyna Macura, M.D., Ph.D.**[1], **Pedram Argani, M.D.**[2,3], **Nagi Khouri, M.D.**[1], **Theodore Tsangris, M.D.**[2], **Peter B. Barker, D.Phil**[1], **Nancy E. Davidson, M.D.**[2,4], **Zaver M. Bhujwalla, Ph.D.**[1,2], **David A. Bluemke, M.D., Ph.D.**[1], and **Ronald Ouwerkerk, Ph.D.**[1]

[1] Russell H. Morgan Department of Radiology and Radiological Sciences, The Johns Hopkins University School of Medicine, Baltimore, MD 21205

[2] Sidney Kimmel Comprehensive Cancer Center, The Johns Hopkins University School of Medicine, Baltimore, MD 21205

[3] Department of Pathology, The Johns Hopkins University School of Medicine, Baltimore, MD 21205

Abstract

Rationale and Objectives—We conducted a prospective study to investigate using multiparametric and multinuclear magnetic resonance imaging(MRI) during preoperative systemic treatment(PST) for locally advanced breast cancer.

Methods—Women with operable stage II or III breast cancer who received PST were studied using dynamic-contrast-enhanced(DCE)-MRI, spectroscopy(MRS), and (^{23}Na)sodium MR. Quantitative metrics of choline peak signal-to-noise ratios(SNR), total sodium concentration(TSC;mM), tumor volumes and Response Evaluation Criteria In Solid Tumors (RECIST) were determined and compared to final pathological result with ROC analysis. Hormonal markers were investigated. Statistical significance was set at $p<0.05$.

Results—Eighteen(n=18) eligible women were studied. Fifteen(n=15) responded to therapy, four(22%) with pathological-complete-response(pCR) and eleven(61%) with a pathological-partial-response(pPR). Three patients(17%) had no response(pNR). Among ER+, HER2+, and Triple Negative(TN) phenotypes, observed frequencies of pCR, pPR, and pNR were 2/5/0, 1/4/0, and 1/1/3, respectively. Responders(pCR and pPR) had the largest reduction in choline SNR (35%:7.2±2.3 to 4.6±2;p<0.01) compared to pNR(11%:8.4±2.7 to 7.5±3.6;p=0.13) after the first cycle. TSC significantly decreased in responders(27%:66±18 to 48.4±8mM;p=0.01), while there was little change in non-responders(51.7±7.6 to 56.5±1.6;p=0.50). Lesion volume decreased in responders(40%:78±78 to 46±51mm^3;p=0.01) and nonresponders(21%:100±104 to 79.2±87 mm^3;p=0.23) after the first cycle. The largest reduction in RECIST occurred after the first treatment in responders(18%:24.5±20 to 20.2±18mm;p=0.01) with a slight decrease in tumor diameter noted in nonresponders(17%;23±19 to 19.2±19.1mm;p=0.80).

Address Correspondence To: Michael A. Jacobs, Ph.D., Department of Radiology, The Johns Hopkins University School of Medicine, Traylor Blg, Rm 217, 712 Rutland Ave, Baltimore, MD 21205, Tel:410-955-7492, Fax:410-614-1948: mikej@mri.jhu.edu.
[4]Present Address: University of Pittsburgh Cancer Institute, Pittsburgh, PA 15232

Conclusion—Multiparametric and Multinuclear imaging parameters were significantly reduced after the first cycle of PST in responders, specifically, Choline SNR and Sodium. These new surrogate radiological biomarkers maybe able to predict and provide a platform for potential adaptive therapy in patients.

Keywords

Breast; Magnetic Resonance Imaging; Sodium MR; ^{23}NA; spectroscopy; proton; Advanced Cancer

INTRODUCTION

Breast cancer is a potentially curable disease, and the combined effects of early detection and adjuvant systemic therapy are likely the key elements that explain the observed reduction in breast cancer mortality over the last 20 years(1). The currently accepted standards for the detection and diagnosis of breast abnormalities are mammography, ultrasound, and magnetic resonance imaging (MRI)(2–3). If breast lesions are detected early, adjuvant systemic therapy after primary surgery reduces the risk of systemic recurrence or death(4–5). However, not all breast cancers are detected early and some patients may present with stage II or III disease and require multi-modality therapy. Preoperative systemic therapy (PST), also referred to as primary or neoadjuvant chemotherapy, is used to potentially reduce the size of the tumor and possibly convert a mastectomy to a lumpectomy in primary operable or locally advanced breast cancer(6–8). Perhaps of greater therapeutic implications, it may allow an early assessment of disease responsiveness and an opportunity to adjust therapy based on observed response(5)

Pathologic response following PST appears to correlate with long-term outcome. National Surgical Adjuvant Bowel and Breast Project (NSABP) trial protocol B18 showed that approximately 12% of patients had a pCR with an anthracycline-based regimen (e.g., doxorubicin and cyclophosphamide - AC)(9), while the addition of four more cycles of a taxane in NSABP-B27 doubled the pCR rate compared to AC alone(10). However, patients who achieved a pCR in these two studies had longer disease-free and overall survival(5). If this is confirmed it implies that, the early identification of those likely to respond to PST becomes of critical importance as a prognostic marker and to potentially allow mid-course adjustments in therapy. Thus, *in vivo* assessment before, during, and after PST may improve decision-making and outcome. Recent studies have demonstrated that an *in vivo* assessment of therapeutic response is possible using MRI in patients who are undergoing PST(11–13). Hylton et al. demonstrated that the use of dynamic contrast-enhanced MRI could be predictive of outcome after a reduction in the size of the tumor in a recent American College of Radiology Imaging Network (ACRIN) multi-institutional center trial(12). Messiamy et al. (14) reported that the use of magnetic resonance spectroscopy (MRS) within 24–48hrs after the first cycle of therapy could detect cellular changes in total choline (Cho) concentration within the tumor, and this has been confirmed by others(15–17). In addition, recent reports have demonstrated that the use of ^{23}Na MRI in patients with breast and other diseases provides additional metabolic information for diagnosis(18–20). However, no one has combined all of these advanced MRI methods, which would enable the gathering of information about the metabolic biochemical status of the tumor microenvironment and surrounding tissue in one setting. Knowledge of the state of the tissue and the tumor microenvironment prior to treatment and, ideally, immediately after the first cycle of therapy may be a critical determining factor to evaluate therapeutic efficacy. This information is important because patients who would likely not respond to treatments would still be at increased risk of toxicity from continued treatment. Thus, by integrating MRI, such as

dynamic contrast-enhanced(DCE-MR), MRS, and ^{23}Na imaging, the potential exists for early identification of patients who may or may not respond to therapeutic intervention.

Therefore, our goal is to prospectively investigate the relationship between multiparametric MR parameters and treatment response in patients with operable breast cancer undergoing PST.

METHODS AND MATERIALS

Clinical Subjects

Female patients (n=18, age range:18–80) who had stage II or III breast cancer and were to receive PST were enrolled in this *prospective* study. The patients were imaged before treatment and after biopsy (baseline), after the first cycle (within 14 days), and at the conclusion of PST therapy, but just before surgery. Patients who received PST with an anthracycline-based regimen were studied. The chemotherapy regimen is AC (doxorubicin {60mg/m^2} + cyclophosphamide {600mg/m^2 intravenous (IV)}) every 21 days × 4 cycles (approximately 12 weeks), followed by paclitaxel (175mg/m^2) or docetaxel (100mg/m^2 IV). If Her2-neu receptor positive by FISH, then trastuzumab-containing regimen was added as determined by the treating oncologist.

Pathological Response and Histological Tissue Classification

Initial breast lesion classification was determined by core biopsy after clinical breast imaging (mammography and ultrasound) including MRI. Clinical response was evaluated in the breast and regional lymph nodes. The patient was examined at the time of study enrollment, after each cycle of PST, and prior to surgery. Clinical response of the primary tumor was accomplished by palpitation and measured if possible, and nodes were evaluated by the treating physician at baseline and at the 4th cycle of treatment. All histological tissue analysis were performed or reviewed as part of the patient's routine clinical care by a Breast Pathology at presentation and at surgery. After PST, the lesion was evaluated for pathological response. Pathologic complete response (pCR) was defined as no viable invasive cancer (macro or microscopically) in the pathologic specimen at histological examination. Pathologic partial response (pPR) is defined as a considerable reduction in tumor cells could be detected. Pathologic no but presence of ≤ 10% microscopic foci of invasive cancer cells response (pNR) was defined in specimens that did not meet the criteria for a pathologic complete or partial response.

Immunohistochemistry values were performed to assess the status of hormonal receptors (estrogen and progesterone) and Her2-neu on a *baseline biopsy* and were repeated on the final surgical specimens at the discretion of the pathologist. For analysis, pCR and pPR are grouped as responders and all others as non-responders. The protocol was approved by the local Institutional Review Board, and informed consent was obtained from all subjects.

MR imaging protocol

Proton MR imaging—MRI was performed on a 1.5T scanner (GE Healthcare, Milwaukee, WI) using a 4-channel phased array breast coil(Medrad, Warrendale, PA) with the patient in the prone position. MR sequences were: Sagittal fat suppressed(FS) T_2WI fast spin echo (TR/TE=5700/102), and fast spoiled gradient echo (FSPGR) T_1WI (TR/TE=200/4.4) with an 18–20 × 18–20cm field of view (FOV), slice thickness of 4 mm and 1mm slice gaps, 256 × 192 acquisition matrix. In addition, 3D-FSPGR T_1WI(TR/TE=20/4, 512 × 160 matrix, 2mm slice thickness) pre- and post-contrast-enhanced (DCE) images were obtained after intravenous administration of 0.1 mmol/kg gadodiamide contrast agent (Omniscan, GE Health Systems). The contrast agent was injected over 10 seconds, with MR

imaging beginning immediately after completion of the injection, immediately followed by a 20cc saline flush. Total scan time for the protocol was less than 20 minutes.

Proton MR Spectroscopy

Spectroscopy was performed in a single 10 mm-thick sagittal section using a point-resolved spectroscopy sequence (PRESS) after the completion of MRI(21–22). The section location was defined by a radiologist to include the lesion. MRS parameters were TR/TE=2000/280 ms, 18 × 18matrix size, 18cm FOV, and total acquisition time was 12 minutes. Nominal voxel size was approximately 1.0 cc. The echo signal was digitized with 256 data points and a spectral width of 1000 Hz. Prior to MRS, shimming was performed to optimize field homogeneity. Water suppression was using “CHESS” pulses with a bandwidth of 75 Hz, applied on-resonance with the water signal(23). Lipid signals were attenuated by using an inversion pulse (STIR) with a delay of 171ms.

^{23}Na Sodium MRI

For quantitative ^{23}Na MRI, subjects were positioned in a custom-made ^{23}Na transmit/receive three turn solenoid breast coil inserted in the ^{1}H MR breast coil. The coil contained a ring shaped phantom containing a 100 mmol/l NaCl solution as both a signal reference and fiducial marker for optimal registration with ^{1}H images. A projection imaging sequence was used with a TR of 100ms, an ultrashort TE=0.2 ms, and 400μs adiabatic excitation pulses. The resolution was 6mm isotropic (0.2 ml voxel volume), with a 22 cm FOV interpolated to 128 × 128 points by 64 slices (3.4 mm slice and 1.7 × 1.7mm in-slice resolution).

MR Image Preprocessing and Analysis

Lesion and Volume Analysis—Clinical analysis was performed using RECIST criteria on measurable lesions (i.e. longest diameter>10mm)(24–25). MR analysis was performed using a SUN T2000 workstation (Sun Microsystems Inc., Mountain View, CA.) with the Eigentool image analysis software (Image Analysis Lab, Henry Ford Hospital, Detroit MI) (26). Volumes were obtained from the subtracted DCE-MR images by thresholding and morphological operators. Threshold ranges were determined using histogram analysis from regions of interest (ROI) placed around the identified lesion using 95% confidence intervals determined from signal intensity within the ROI. Finally, reproducibility estimates (inter and intra-variability) were determined of the lesion boundaries. Representative DCE-MR images during treatment are shown in Figure 1.

Magnetic Resonance Spectroscopy Analysis—Spectroscopy data were reconstructed using in-house software on a Sun T2000 (Sun Microsystems Inc., Mountain View, CA.). The data sets were processed by 3D Fourier transformation, with cosine filters in the spatial (phase-encoding) domains after zero-filling to 32 × 32 matrix size, and exponential line broadening of 3Hz, zero-filling to 2048 data points, and a high-pass convolution filter to remove the residual water signal (50Hz stop-band) in the time domain. After setting the chemical shift of water to 4.7ppm, chemical shifts measurements were performed on the choline (Cho, 3.34 to 3.14 ppm). The peak height of the signal in the Cho frequency range in one voxel localized completely within the lesion was quantified using a simplex curve-fitting routine and expressed as a ratio relative to the background noise level between 7.0 and 9.0 ppm (where no signals are expected) in the same voxel. The criteria for determining the presence or absence of Cho were that a peak height should be clearly identifiable above baseline noise at 3.2ppm (SNR>4)(27–28).

Quantitative ^{23}Na Sodium MRI—The ^{1}H MR images were co-registered with the ^{23}Na images using software developed in-house with Matlab(Mathworks, Natick, MA). Intensity

contours are copied between co-registered images to guide the placement of ROI's on the ^{23}Na images to determine the TSC, signal-to-noise ratio (SNR), and contrast-to-noise ratio (CNR). The TSC in breast and other tissue was determined as previously described(19–20,27,29–30).

Statistical Analysis

The differences in MR-defined DCE volumes, RECIST measurements, choline SNR, and ^{23}Na concentrations before and after treatment were evaluated using a 2-sided paired t-test and ANOVA and compared with final pathological result. Receiver operating characteristic (ROC) curve analysis was performed to assess the diagnostic performance of the radiological parameters in characterizing responders versus non-responders and determine the area under the ROC curve(AUC). Statistical significance was set at $p<0.05$.

RESULTS

Clinical and Histopahtological Characteristics

18 patients (median±SD:49±8, range=18–60) who met eligibility criteria and signed a written informed consent were enrolled in this study over a four period. Ten (56%) patients were premenopausal and eight (44%) were postmenopausal and the summary statistics of clinical parameters are shown in Table 1. All 18 patients had baseline MRI imaging, 18 had subsequent imaging after one week/cycle and 14 had final imaging after completion of PST (before surgery). 11 patients received AC followed by a taxane chemotherapy, while 7 received taxane followed AC. Five patients had HER2-positive disease and 5 were treated with a trastuzumab-containing regimen.

Clinical Response and Pathology Findings after PST

During treatment, four patients had cCR, five patients had cPR, and five patients had progressive and/or stable disease. In four patients, clinical response was not determined. All 18 patients had surgery after PST. 28% (n=5) had a pCR with no residual invasive cancer in the breast and axilla, while 55% (n=10) had a pPR and 17% (n=3) had a pNR. Among ER+, HER2+, and Triple Negative (TN) phenotypes, the observed frequencies of pCR, pPR, and pNR were 2/5/0, 1/4/0, and 1/1/3, respectively.

Radiological Metrics

General—Figure 1 demonstrates the ability of DCE-MR to define the extent of disease, vascularity, and monitor tumor response throughout the course of treatment. Figure 2 demonstrates the use of multiparametric and multinuclear imaging and shows the potential to obtain different, yet complementary information of the tumor microenvironment during therapeutic intervention. Indeed, changes in the radiological metrics before, during, and after treatment show differences in choline MRS, ^{23}Na, and the DCE-MR, indicating that, by combining these methods, more information was obtained, this patient has a pCR. Similarly, Figure 3 demonstrates the lack of changes in radiological metrics during treatment was a non-responder (pNR) patient at surgical presentation.

RECIST—The largest reduction in RECIST occurred after the first treatment in the responder group with a decrease in diameter of the lesion by 18% (24.5±20 to 20.2±18mm;p=0.01). There was a decrease in tumor diameter noted in the nonresponders (17%;23±19 to 19.2±19.1mm;p=0.80). The AUC for RECIST at baseline was 0.67(p=0.49) and after the first cycle was 0.56(p=0.81).

MR Spectroscopy—The largest reduction in choline SNR occurred after the first treatment in both groups. However, the greatest decline in choline SNR (35%) was noted in the responder group (7.2±2.3 to 4.6±2;p<0.01) after the first cycle (day3–7) of treatment, with a smaller decline (11%) in choline SNR in non-responders (8.4±3 to 7.5±3.6;p=0.13), as shown in Figure 4. The choline SNR was only slightly decreased (before surgery in both groups, suggesting that the treatment effect on tumors is greatest during the initial treatment cycles (Figure 4). In addition, there is a loss of spectral resolution of the choline signal at the time of surgery. The AUC for choline SNR at baseline was 0.71(p=0.18) and after the first cycle was 0.82(p=0.09).

^{23}Na Sodium—The total sodium concentration (TSC) in breast tumors decreased in responders (27%:66±18 to 48.4±8mM;p=0.01) and did not change (52±8 to 56±2;p=0.50) in the non-responders (pNR) after the first cycle (figure 4). However, there were decreases in the TSC during the final treatment cycles for both groups. The AUC for Sodium TSC at baseline was 0.79 (p=0.009) and after the first cycle was 0.83(p=0.003).

Proton DCE-MR—Mean DCE MR tumor volume decreased between baseline and the first cycle of treatment in both groups of patients, with the largest decrease in the responders (40%:78±78 to 46±51mm^3;p=0.01) and pNR (21%:100±104 to 79.2±87 mm^3;p=0.23) after the first cycle(figure 4). The volume continued to significantly decrease in responders and only slightly decrease in pNR until the end of treatment. However, there was a large variability in the size of the tumors. The AUC for MR volumes at baseline was 0.75(p=0.06) and after the first cycle was 0.73(p=0.14).

Subgroup Analysis between Pathologic Response, Tumor Phenotype, and Imaging Findings Triple Negatives—The patients with TN phenotypes (n=5) had varied pathological response, two had cPR and three were nPR. Interesting, the changes in choline SNR, TSC and volumes were greatest after the first cycle in the cPR (46%, 26%, and 34%, respectively) compared to pNR (17%, −9% and 16%, respectively).

ER-/PR-, HER2+—The ER-/PR-, HER2+ group, the largest decline was in choline SNR (62%) and volume (43%) with a 26% decrease in TSC after the first cycle.

ER+/PR+/HER2—Lastly, the ER+/PR+/HER2- exhibited similar radiological metrics after treatment as the ER-/PR-, HER2+, except the largest decline was in volumetrics(49%), followed by choline SNR(37%) and TSC(17%). Both of these groups of patients were responders(pPR).

Discussion

We have demonstrated the feasibility of using multiparametric and multinuclear proton, MRS, and ^{23}Na MR imaging for monitoring PST in patients with operable breast cancer in the clinical setting. Significant decreases in choline SNR and total sodium concentration (TSC) were observed in responders after the first cycle of treatment with higher AUC. Conversely, stable TSC with smaller decreases in choline SNR were noted in non-responders after the first cycle of treatment with lower AUC. These data suggest that these radiological imaging markers could be indicative of tissue response or lack of response after initial treatment. This is the first clinical study to employ *combined* multiparametric and multinuclear MR studies for monitoring treatment response. Indeed, by combining advanced MRI methods, important biophysical information, beyond standard morphologic or volumetric data, can be obtained about the tumor microenvironment and this will provide a basis for radiological procedures that could be utilized as surrogate biomarkers in

conjunction with tumor phenotype for monitoring therapeutic intervention. Specifically, by examining changes in TSC and choline MRS, the tumor and local microenvironment can be investigated before changes are noted using traditional response criteria, such as Response Evaluation Criteria in Solid Tumors (RECIST) and provide a platform for adaptive therapy.

Therapeutic changes occur within tumor cells and determining when and if disruptions of the metabolic/biochemical pathways have occurred is of major importance, both clinically and economically. Most PST is cytotoxic in nature and will induce changes in the tumor cellular membrane with the hope to disrupt intra- and extra-cellular function of tumor cells. Any disruption of these pathways in the cell will affect the intracellular sodium concentration (ICS) and membrane permeability. This will lead to an increase in TSC(31–33) Sodium concentration is a sensitive indicator of cellular integrity and may, therefore, be useful in assessing therapeutic response to interventions that disrupt cellular structure such as targeted therapeutics in preclinical models(34–36). However, there have been no clinical applications to date using all these methods.

Our work demonstrates that ^{23}Na MRI methods appear to have potential value for the assessment of treatment response and may reflect differences tumor phenotypes in the clinical setting. The sodium TSC had the highest AUC for correct prediction of treatment response. We noted large decreases in the TSC of patients that were TN or only HER+ and were responders, whereas, in non-responder patients with similar hormonal status, no or little changes in TSC concentrations were shown. Presumably, if the tumor responds to treatment, there should be a decrease in the proliferation of tumor cells, which would lead to a normalization of sodium homeostasis and no further increase in extracellular space and/or vascularization. If there is no response to treatment, continued proliferation of tumor cells involves more processes that are competing for ATP with the Na^+/K^+ pump, and the higher demands for ATP and altered cation homeostasis will create changes in the microenvironment which may prompt a further increase in vascularization. This leads to changes predominately in intracellular component and less in the extracellular sodium component that may result in increased TSC(34). However, to fully understand the effect of PST on patients using ^{23}Na MR, multiple quantum filter (MQF) methods are need to separate the intra and extracellular components(37–40).

Spectroscopy can demonstrate metabolic differences between normal tissue and tumor environments based on the presence or absence of a choline peak. Choline compounds are total choline (consisting of phosphocholine(PC), glycerophosphocholine(GPC) and free choline (Cho)). Typically, malignant tumors exhibit elevated levels of phosphocholine mostly due to increased expression and activity of choline kinase, the enzyme that converts free choline to phosphocholine(41). Tumors with high phosphocholine are presumably more aggressive and more resistant to chemotherapy, such as TN phenotypes(42–43). Thus, changes in choline SNR have been shown to occur within 24–48 hrs after treatment in PST treatment and correlate with a positive response(14–17). However, the lack of changes in choline after treatment has been associated with an unfavorable response. Indeed, in our study, patients with TN and only HER2+ phenotypes had the smallest decrease in choline SNR after treatment. Whereas, patients with ER+/PR+ phenotype had greatest decline in choline SNR after treatment. However, the choline AUC for correct prediction of response was slightly smaller than the TSC for correct prediction of response (0.82 vs. 0.83). As expected, RECIST measurement were the demonstrated the lowest AUC for predicating outcome since morphologic changes are known the change at the later stages of PST. But, RECIST methods are the easiest to implement and are widely used.

There are, however, some technical limitations to the use of ^{23}Na imaging and MRS. First, although the use of ^{23}Na MRI is now finding some applications in the brain, breast, uterus,

and heart(18–20,29), the multinuclear hardware and ultra-short TE pulse sequences used here are not widely available as of yet. Also, the ability to separate the intracellular from extracellular component would provide more information to what is occurring in the different tumor compartments. To separate the intracellular from the extracellular spaces MQF is needed due the 3/2 spin of the sodium ion(37–40). The use of MQF currently under active research and was not feasible in this study. In addition, a direct correlation to histology is needed to validate the radiopathological findings. Second, we utilized the choline SNR as a quantification measure, which measures peak height, but a more accurate method of choline quantification is needed. There are several methods using either internal or external reference or a phantom replacement model(44–47). We are currently implementing the phantom replacement method for all patients undergoing MRS interrogation. Finally, these results are preliminary and any assessment of the clinical value of multiparametric proton, MRS, and ^{23}Na MRI in monitoring treatment response of PST will require additional studies in a larger patient population, with subsequent follow-up with histological and phenotype evaluation to discern the sensitivity and specificity of this approach and the exact mechanisms underlying these changes. Also, the addition of diffusion weighted imaging/Apparent Diffusion Coefficient (ADC) mapping and pharmacokinetic DCE modeling of the vascular will bring additional parameters and increase tissue characterization(48–51)

In conclusion, we have demonstrated that advanced radiological imaging is feasible to monitor PST in breast cancer patients. These methods might be used for surrogate endpoint biomarkers to rapidly predict response to PST. Promising surrogate radiological biomarkers of response to therapy include total sodium concentration and choline measurements.

Acknowledgments

We thank all the patients for participating in these studies. We are grateful for the help of Mary McAllister, MA., Lucie Bower, Dr Donald Peck, and Dr. Hamid Soltanian-Zadeh, Henry Ford Hospital, Detroit, MI for the Eigentool image analysis software used for image processing.

References

1. Jemal A, Siegel R, Ward E, et al. Cancer statistics, 2009. CA Cancer J Clin. Jul–Aug; 2009 59(4): 225–249. [PubMed: 19474385]
2. Lehman CD, Gatsonis C, Kuhl CK, et al. MRI evaluation of the contralateral breast in women with recently diagnosed breast cancer. N Engl J Med. Mar 29; 2007 356(13):1295–1303. [PubMed: 17392300]
3. El Khouli RH, Jacobs MA, Bluemke DA. Magnetic resonance imaging of the breast. Semin Roentgenol. Oct; 2008 43(4):265–281. [PubMed: 18774031]
4. Effects of chemotherapy and hormonal therapy for early breast cancer on recurrence and 15-year survival: an overview of the randomised trials. Lancet. May 14–20; 2005 365(9472):1687–1717. [PubMed: 15894097]
5. Wolff AC, Berry D, Carey LA, et al. Research issues affecting preoperative systemic therapy for operable breast cancer. J Clin Oncol. Feb 10; 2008 26(5):806–813. [PubMed: 18258990]
6. Fisher B, Redmond C, Brown A, et al. Adjuvant chemotherapy with and without tamoxifen in the treatment of primary breast cancer: 5-year results from the National Surgical Adjuvant Breast and Bowel Project Trial. J Clin Oncol. 1986; 4(4):459–471. [PubMed: 2856857]
7. Fisher B, Redmond C, Wickerham DL, et al. Systemic therapy in patients with node-negative breast cancer. A commentary based on two National Surgical Adjuvant Breast and Bowel Project (NSABP) clinical trials. Ann Intern Med. 1989; 111(9):703–712. [PubMed: 2679288]
8. Kaufmann M, Hortobagyi GN, Goldhirsch A, et al. Recommendations from an international expert panel on the use of neoadjuvant (primary) systemic treatment of operable breast cancer: an update. J Clin Oncol. Apr 20; 2006 24(12):1940–1949. [PubMed: 16622270]

9. Fisher B, Bryant J, Wolmark N, et al. Effect of preoperative chemotherapy on the outcome of women with operable breast cancer. J Clin Oncol. 1998; 16(8):2672–2685. [PubMed: 9704717]
10. NSABP. The effect on primary tumor response of adding sequential Taxotere to Adriamycin and cyclophosphamide: preliminary results from NSABP Protocol B-27. Breast Cancer Res Treat. 2001; 69(210):215.
11. Esserman L, Hylton N, Yassa L, et al. Utility of magnetic resonance imaging in the management of breast cancer: Evidence for improved preoperative staging. Journal of Clinical Oncology. 1999; 17(1):110–119. [PubMed: 10458224]
12. Partridge SC, Gibbs JE, Lu Y, et al. MRI measurements of breast tumor volume predict response to neoadjuvant chemotherapy and recurrence-free survival. AJR Am J Roentgenol. Jun; 2005 184(6): 1774–1781. [PubMed: 15908529]
13. Yu HJ, Chen JH, Mehta RS, et al. MRI measurements of tumor size and pharmacokinetic parameters as early predictors of response in breast cancer patients undergoing neoadjuvant anthracycline chemotherapy. J Magn Reson Imaging. Sep; 2007 26(3):615–623. [PubMed: 17729334]
14. Meisamy S, Bolan PJ, Baker EH, et al. Neoadjuvant Chemotherapy of Locally Advanced Breast Cancer: Predicting Response with in Vivo 1H MR Spectroscopy--A Pilot Study at 4 T. Radiology. 2004; 233(2):424–431. [PubMed: 15516615]
15. Manton DJ, Chaturvedi A, Hubbard A, et al. Neoadjuvant chemotherapy in breast cancer: early response prediction with quantitative MR imaging and spectroscopy. Br J Cancer. 2006; 94(3): 427–435. [PubMed: 16465174]
16. Kumar V, Jagannathan NR, Kumar R, et al. Correlation between metabolite ratios and ADC values of prostate in men with increased PSA level. Magn Reson Imaging. 2006; 24(5):541–548. [PubMed: 16735174]
17. Baek HM, Chen JH, Nie K, et al. Predicting pathologic response to neoadjuvant chemotherapy in breast cancer by using MR imaging and quantitative 1H MR spectroscopy. Radiology. 2009; 251(3):653–662. [PubMed: 19276320]
18. Jacobs MA, Ouwerkerk R, Wolff AC, et al. Multiparametric and multinuclear magnetic resonance imaging of human breast cancer: current applications. Technol Cancer Res Treat. 2004; 3(6):543–550. [PubMed: 15560711]
19. Ouwerkerk R, Jacobs MA, Macura KJ, et al. Elevated tissue sodium concentration in malignant breast lesions detected with non-invasive (23)Na MRI. Breast Cancer Res Treat. Jan 27; 2007 106(2):151–160. [PubMed: 17260093]
20. Jacobs MA, Ouwerkerk R, Kamel I, et al. Proton, diffusion-weighted imaging, and sodium ((23)Na) MRI of uterine leiomyomata after MR-guided high-intensity focused ultrasound: A preliminary study. J Magn Reson Imaging. Feb 25; 2009 29(3):649–656. [PubMed: 19243047]
21. Bottomley PA. Spatial localization in NMR spectroscopy in vivo. Ann N Y Acad Sci. 1987; 508:333–348. [PubMed: 3326459]
22. Jacobs MA, Barker PB, Bluemke DA, et al. Benign and malignant breast lesions: diagnosis with multiparametric MR imaging. Radiology. 2003; 229(1):225–232. [PubMed: 14519877]
23. Haase A, Frahm J, Hanicke W, et al. H-1-Nmr Chemical-Shift Selective (Chess) Imaging. Physics in Medicine and Biology. 1985; 30(4):341–344. [PubMed: 4001160]
24. Therasse P, Eisenhauer EA, Verweij J. RECIST revisited: a review of validation studies on tumour assessment. Eur J Cancer. May; 2006 42(8):1031–1039. [PubMed: 16616487]
25. Eisenhauer EA, Therasse P, Bogaerts J, et al. New response evaluation criteria in solid tumours: Revised RECIST guideline (version 1.1). European Journal of Cancer. 2009; 45(2):228. [PubMed: 19097774]
26. Jacobs MA, Knight RA, Windham JP, et al. Identification of cerebral ischemic lesions in rat using eigenimage filtered magnetic resonance imaging. Brain Research. 1999; 837(1–2):83–94. [PubMed: 10433991]
27. Jacobs MA, Barker PB, Bottomley PA, et al. Proton MR spectroscoptic imaging of human breast cancer:a preliminary study. Journal of Magnetic Resonance Imaging. 2004; 19(1):68–75. [PubMed: 14696222]

28. Baek HM, Yu HJ, Chen JH, et al. Quantitative correlation between (1)H MRS and dynamic contrast-enhanced MRI of human breast cancer. Magn Reson Imaging. May; 2008 26(4):523–531. [PubMed: 18060716]
29. Ouwerkerk R, Bleich KB, Gillen JS, et al. Tissue sodium concentration in human brain tumors as measured with 23Na MR imaging. Radiology. 2003; 227(2):529–537. [PubMed: 12663825]
30. Ouwerkerk R, Weiss RG, Bottomley PA. Measuring human cardiac tissue sodium concentrations using surface coils, adiabatic excitation, and twisted projection imaging with minimal T2 losses. J Magn Reson Imaging. 2005; 21(5):546–555. [PubMed: 15834912]
31. Hilal SK, Maudsley AA, Ra JB, et al. In vivo NMR imaging of sodium-23 in the human head. J Comput Assist Tomogr. 1985; 9(1):1–7. [PubMed: 3968256]
32. Nagy I, Lustyik G, Lukacs G, et al. Correlation of malignancy with the intracellular Na+:K+ ratio in human thyroid tumors. Cancer Res. 1983; 43(11):5395–5402. [PubMed: 6616471]
33. Navon G. Complete elimination of the extracellular 23Na NMR signal in triple quantum filtered spectra of rat hearts in the presence of shift reagents. Magn Reson Med. 1993; 30(4):503–506. [PubMed: 8255200]
34. Kline RP, Wu EX, Petrylak DP, et al. Rapid in vivo monitoring of chemotherapeutic response using weighted sodium magnetic resonance imaging. Clin Cancer Res. 2000; 6(6):2146–2156. [PubMed: 10873063]
35. Winter PM, Poptani H, Bansal N. Effects of Chemotherapy by 1,3-Bis(2-chloroethyl)-1-nitrosourea on Single-Quantum- and Triple-Quantum-filtered 23Na and 31P Nuclear Magnetic Resonance of the Subcutaneously Implanted 9L Glioma. Cancer Res. 2001; 61(5):2002–2007. [PubMed: 11280759]
36. Babsky AM, Topper S, Zhang H, et al. Evaluation of extra- and intracellular apparent diffusion coefficient of sodium in rat skeletal muscle: effects of prolonged ischemia. Magn Reson Med. 2008; 59(3):485–491. [PubMed: 18306401]
37. Pike MM, Frazer JC, Dedrick DF, et al. 23Na and 39K nuclear magnetic resonance studies of perfused rat hearts. Discrimination of intra- and extracellular ions using a shift reagent. Biophys J. 1985; 48(1):159–173. [PubMed: 4016206]
38. Pekar J, Renshaw PF, Leigh JS. Selective Detection of Intracellular Sodium by Coherence-Transfer Nmr. Journal of Magnetic Resonance. 1987; 72(1):159–161.
39. Winter PM, Bansal N. Triple-Quantum-Filtered 23Na NMR Spectroscopy of Subcutaneously Implanted 9L Gliosarcoma in the Rat in the Presence of TmDOTP5- Journal of Magnetic Resonance 9. 2001; 152(1):70–78.
40. Tanase C, Boada FE. Triple-quantum-filtered imaging of sodium in presence of B(0) inhomogeneities. J Magn Reson. 2005; 174(2):270–278. [PubMed: 15862244]
41. Glunde K, Jacobs MA, Pathak AP, et al. Molecular and functional imaging of breast cancer. NMR Biomed. 2009; 22(1):92–103. [PubMed: 18792419]
42. Glunde K, Jacobs MA, Bhujwalla ZM. Choline metabolism in cancer: implications for diagnosis and therapy. Expert Rev Mol Diagn. Nov; 2006 6(6):821–829. [PubMed: 17140369]
43. Negendank W, Li CW, Padavic-Shaller K, et al. Phospholipid metabolites in 1H-decoupled 31P MRS in vivo in human cancer: implications for experimental models and clinical studies. Anticancer Res. May–Jun; 1996 16(3B):1539–1544. [PubMed: 8694523]
44. Soher BJ, van Zijl PC, Duyn JH, et al. Quantitative proton MR spectroscopic imaging of the human brain. Magn Reson Med. 1996; 35(3):356–363. [PubMed: 8699947]
45. Bolan PJ, Meisamy S, Baker EH, et al. In vivo quantification of choline compounds in the breast with 1H MR spectroscopy. Magn Reson Med. Dec; 2003 50(6):1134–1143. [PubMed: 14648561]
46. Baik HM, Su MY, Yu H, et al. Quantification of choline-containing compounds in malignant breast tumors by 1H MR spectroscopy using water as an internal reference at 1.5 T. Magma. May; 2006 19(2):96–104. [PubMed: 16779565]
47. Fayad LM, Salibi N, Wang X, et al. Quantification of muscle choline concentrations by proton MR spectroscopy at 3 T: technical feasibility. AJR Am J Roentgenol. Jan; 2010 194(1):W73–79. [PubMed: 20028894]
48. Woodhams R, Matsunaga K, Iwabuchi K, et al. Diffusion-weighted imaging of malignant breast tumors: the usefulness of apparent diffusion coefficient (ADC) value and ADC map for the

detection of malignant breast tumors and evaluation of cancer extension. J Comput Assist Tomogr. Sep–Oct; 2005 29(5):644–649. [PubMed: 16163035]

49. El Khouli RH, Macura KJ, Barker PB, et al. Relationship of temporal resolution to diagnostic performance for dynamic contrast enhanced MRI of the breast. J Magn Reson Imaging. Nov; 2009 30(5):999–1004. [PubMed: 19856413]
50. Jin G, An N, Jacobs MA, Li K. The role of parallel diffusion-weighted imaging and apparent diffusion coefficient (ADC) map values for evaluating breast lesions: preliminary results. Acad Radiol. Apr; 2010 17(4):456–463. [PubMed: 20207316]
51. El Khouli RH, Jacobs MA, Macura KJ, et al. Diffusion Weighted Imaging Improves the Diagnostic Accuracy of Conventional Breast MRI at 3 Tesla. Radiology. 2010; 1(256):64–73.

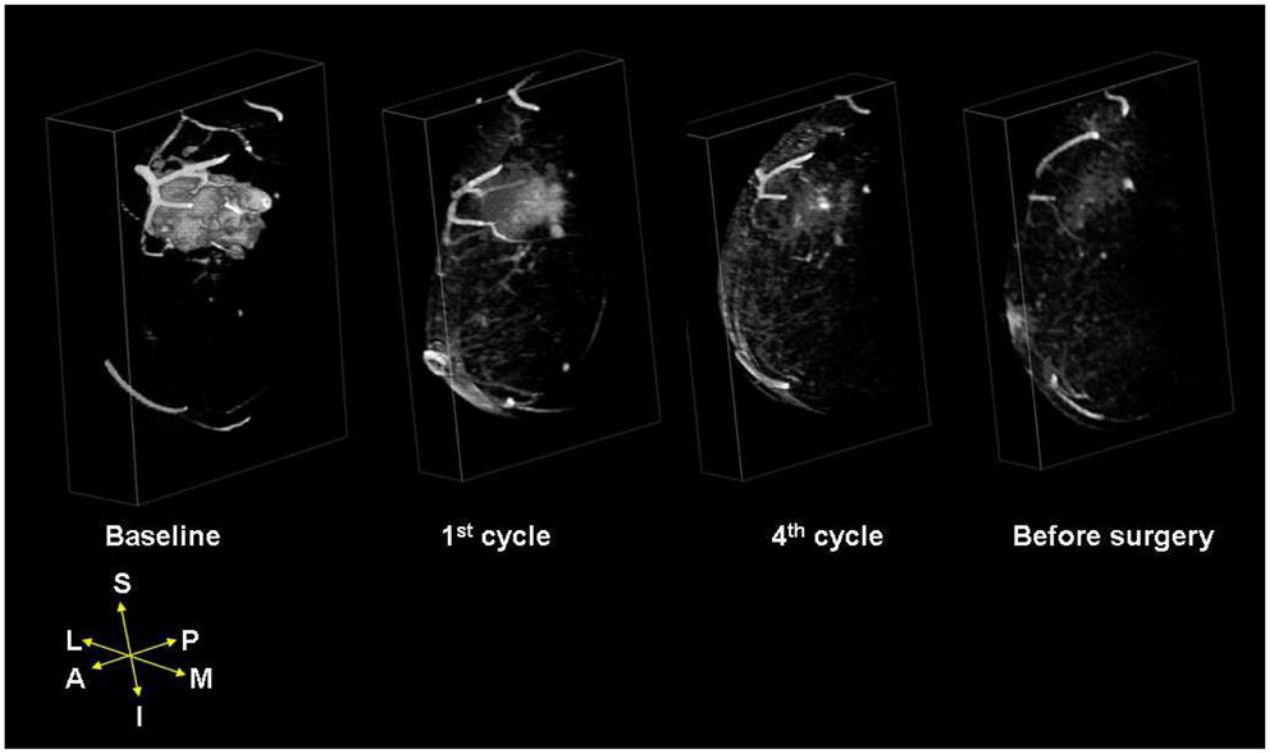

Figure 1.
Representative 3D visualization of dynamic contrast-enhanced MR images after therapeutic intervention in a 54 y/o female with T3N0M0 invasive ductal carcinoma of a large operable breast lesion. There was a steady reduction in tumor volume from baseline until surgery.

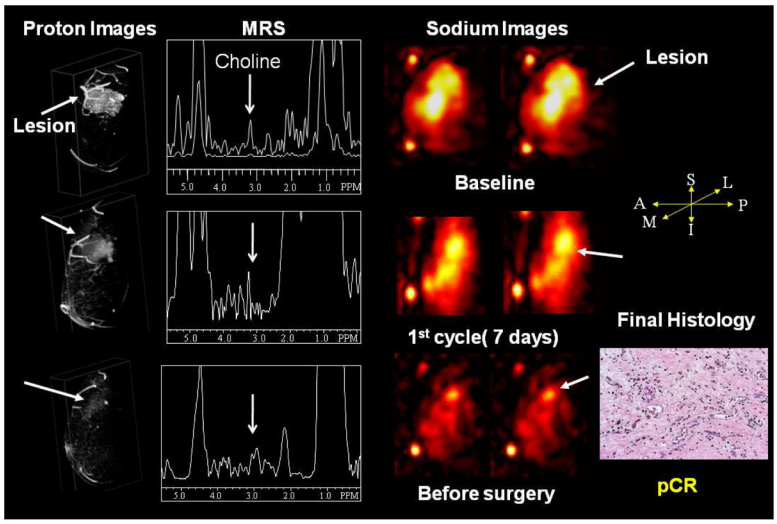

Figure 2.

Demonstration of multiparametric and multinuclear MR on a 54 y/o female with T3N0M0 invasive ductal carcinoma receiving doxorubicin and cyclophosphamide followed by docetaxel chemotherapy. At baseline, Choline and Total Sodium Concentration (TSC) was marked increased of contrast in the large tumor volume. After treatment, there was a steady reduction in choline SNR, TSC, and tumor volumes beginning after the first cycle of treatment. At surgery, she was determined to have a complete pathological response.

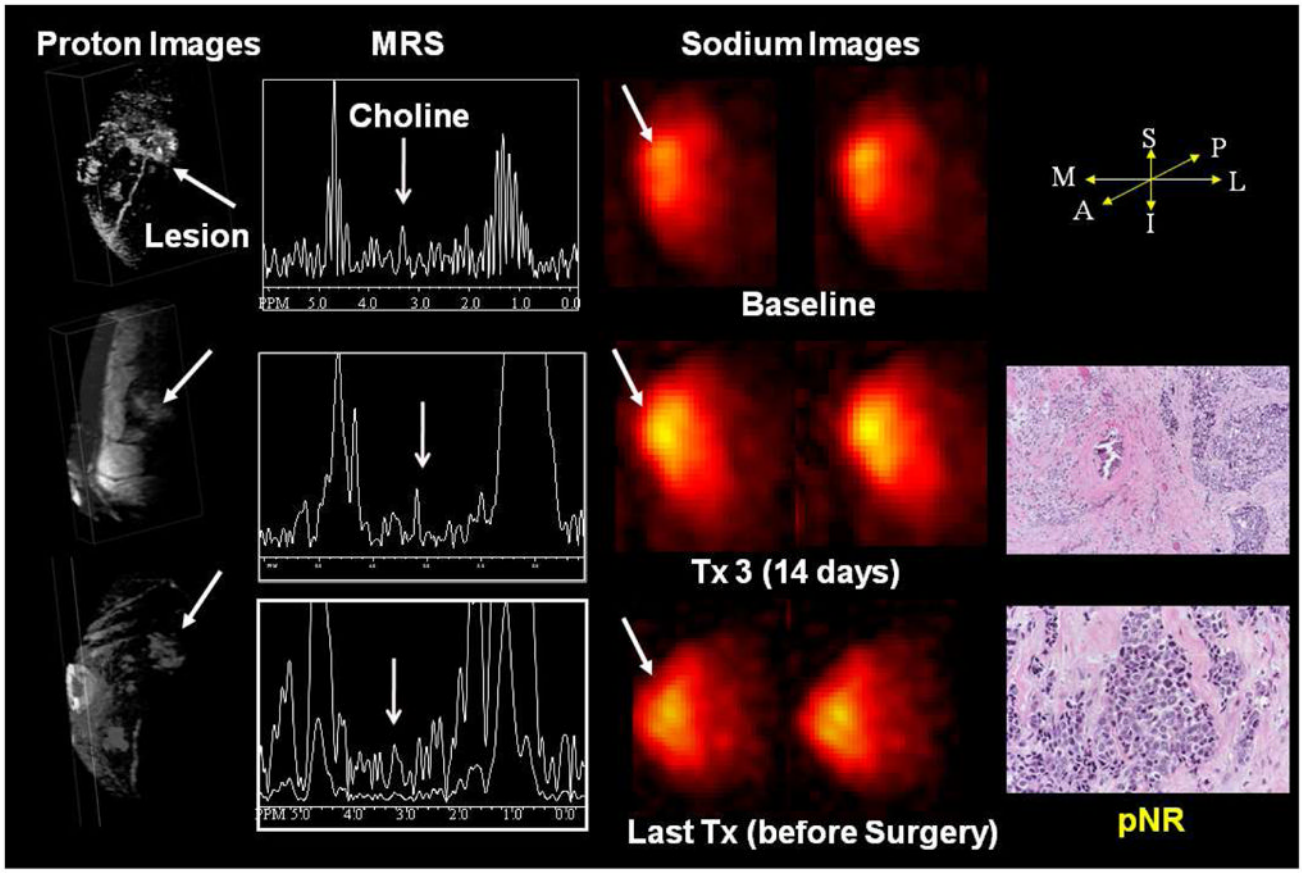

Figure 3.

A representative 49 y/o postmenopausal female with cT2N1M0 invasive ductal carcinoma who was receiving preoperative chemotherapy. **Left column**) DCE-MR showed little or no reduction in tumor volume after treatment. **Middle column:** there is a visible choline peak at 3.2 ppm and it remained constant during the course of treatment. **Right column**: Similarity, there was little change in the sodium intensity and TSC during the course of treatment. Her final pathological diagnosis was pathological no response (pNR) with residual tumor present in the final surgical specimen.

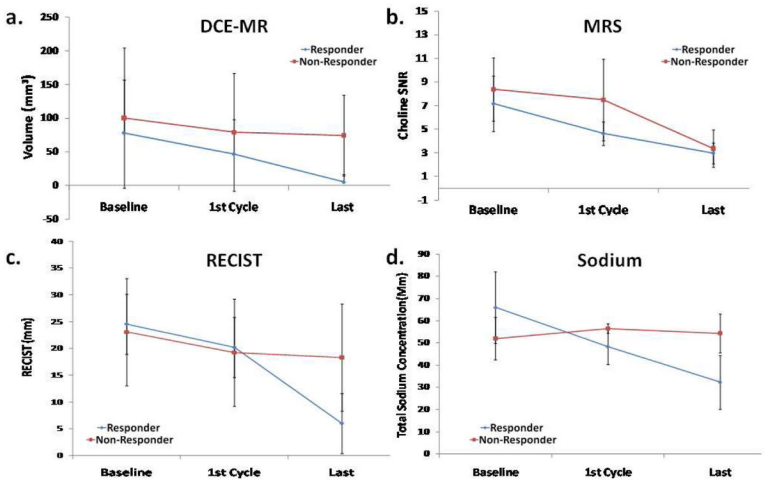

Figure 4.

Line plots of Dynamic Contrast Enhanced (DCE) volumes, Choline signal to noise ratio (SNR), RECIST, and Total (^{23}NA) sodium concentration between responders (cPR and pCR) and non-responders (nPR) for complete PST in patients. The largest reduction in DCE-MR, Cho-SNR, and TSC occurred after the first cycle in responders compared with non-responders. Afterwards, the reductions in DCE-MR, Cho-SNR generally stabilized in both groups, whereas RECIST and TSC continued to decrease in responders until PST was completed and final surgery performed.

Table 1

Patient Characteristics and Treatment Response

Enrolled patients		18
Age, years		
Median	49	
Range	35–68	
Stage (TNM)		
II		4
III		14
Histology		
Ductal		14
Lobular		4
Mixed ductal and lobular		3
Tumor Grade		
2		4
3		14
Estrogen-receptor positive		10
Progesterone-receptor positive		7
Her2-*neu* positive		
IHC (3+)		5
FISH positive		5
Radiological Measures compared to Pathological Response (ROC-AUC)	Baseline	1st cycle
RESICT	0.67	0.56
Sodium	0.79	0.83
Choline	0.71	0.82
DCE-Volume	0.75	0.73

Abbreviations: AUC=Area under the ROC Curve, IHC, immunohistochemistry; FISH, fluorescence in situ hybridization.